Dielectric Relaxation in Vinylidene Fluoride–Hexafluoropropylene Copolymers

Valentin V. Kochervinskii,[1] Inna A. Malyshkina,[2] Grigory V. Markin,[2] Nadezhda D. Gavrilova,[2] Natalia P. Bessonova[3]

[1]*State Research Center of the Russian Federation Troitsk Institute for Innovations and Fusion Research, 142190 Troitsk, Moscow Region, Russia*
[2]*Department of Physics, Moscow State University, 119992 Leninskie Gory, Moscow, Russia*
[3]*State Research Center of the Russian Federation Karpov Institute of Physical Chemistry, Vorontsovo Pole 10, 103064 Moscow, Russia*

Received 20 September 2006; accepted 18 December 2006
DOI 10.1002/app.26145
Published online 10 April 2007 in Wiley InterScience (www.interscience.wiley.com).

ABSTRACT: The molecular mobility in copolymers of vinylidene fluoride–hexafluoropropylene VDF/HFP of 93/7 and 86/14 ratios has been investigated by means of broadband dielectric relaxation spectroscopy (10^{-1}–10^{7} Hz), differential scanning calorimetry DSC (−100 to 150°C), and of wide angle X-ray diffraction WAXS. Four relaxation processes and one ferroelectric-paraelectric phase transition have been detected. The process of the local mobility β- (at temperatures below glass transition point) is not affected by chemical composition of the copolymer and the formed structure. Parameters of segmental mobility in the region of glass transition (α_a-relaxation) depend on the ratio of comonomer with lower kinetic flexibility. α_c-relaxation is clearly observed only in VDF/HFP 93/7 copolymer, which is characterized by a higher crystallinity and a higher perfection of crystals of α- (α_p-) phase. Diffuse order–disorder relaxor type ferroelectric transition connected with the destruction of the domains in low-perfect ferroelectric phase in the amorphous regions has been detected for both copolymers. An intensive relaxation process (α-process) was observed for both copolymers in high-temperature region. DSC data shows that it falls on the broad temperature region of α-phase crystals melting. It is considered to be connected with the space charge relaxation. © 2007 Wiley Periodicals, Inc. J Appl Polym Sci 105: 1101–1117, 2007

Key words: fluoropolymers; dielectric properties; glass transition

INTRODUCTION

There are a number of reasons for PVDF and its copolymers to draw particular attention of researchers. Ferroelectricity[1,2] and high piezo- and pyroactivity in these compounds, along with specific properties of polymers, allow to use them as a material for various energy converters.[3,4] Mechanisms of ferroelectricity and piezoelectricity are still not clearly understood,[2,5,6] particularly the role of molecular mobility in crystalline and especially in the amorphous phase is not clear in these phenomena. Therefore, investigation of mechanisms of molecular dynamics in considered class of polymers is actual.

In the present article, one of the VDF copolymers—with hexafluoropropylene HFP—is being studied. Interest to this object is also stimulated by other reasons. The named copolymer has been used as a component of gel–polymer electrolytes for lithium source of current[7] recently, where it plays a role of a polymer matrix in which lithium ions move. Mobility of such carriers will be determined by intensity of molecular motion in a copolymer. Therefore, the question of mobility characteristics investigations in polymer matrix is actual.

As the basic component of a copolymer is PVDF with strongly pronounced polymorphism,[4,8] it is worth to discuss relaxation processes in this polymer. They were studied both experimentally[9–37] and by computer modeling.[38,39] Appearance of local mobility is registered at temperatures below the glass transition point ($T_g \sim -40$°C) as it was observed in other polymers. It normally follows by one relaxation process, which is usually named as β- or γ-. However, the results in Refs. 20 and 25 show that two more processes are detected at lower temperatures (in different terminology): δ- and ε-[20] or γ_1- and γ_2-.[25] The lowest-temperature one (ε-), for the oriented PVDF with ferroelectric phase, is attributed to the crystals' defects,[20] the amount of which decreases after polarization is applied. The mobility around −40°C is usually connected with the amorphous phase glassing (β-, α_a-transition). The nonlinearity of the relaxation time in the Arrhenius coordinates is typical for this type of transition. It was discovered that the crystallization

Correspondence to: V. V. Kochervinskii (kochval@orc.ru).

Journal of Applied Polymer Science, Vol. 105, 1101–1117 (2007)

process of isotropic films[34,35] and the parameters of their texturing during uniaxial drawing[36,37] are responsible for the local and cooperative α_a-mobility characteristics in case of PVDF and its copolymer with tetrafluoroethylene TFE VDF/TFE of 94/6 ratio. It can be explained qualitatively in the point of view of the latest data on the structure of crystallized polymers. One should differ undisturbed amorphous phase and so-called rigid amorphous phase RAP,[40–42] which can be localized on boundaries of the lamellar crystals. However, there is certain difference in the opinion of authors of Refs. 12 and 28, 29 as to whether the α_a-transition at $\sim -40^\circ$C is ascribed to the former or the latter amorphous phases. Eventually, the results presented in Ref. 12 show that this must be isotropic (undisturbed) amorphous phase, whereas conclusions obtained in Refs. 28, 29 denote that kinetic units must be localized in RAP regions.

PVDF are crystalline polymers, where relaxation type mobility (α_c-) in crystalline phase is generally observed. On the other hand, there is a possibility of formation of ferroelectric phase in this class of polymers.[1,2,4] And therefore in the regions of spontaneous polarization order–disorder transitions are observed.[20,21,25,30] Large number of dielectric measurements illustrate that the α_c-transition is clearly observed in PVDF crystallized in nonpolar phase, but practically disappears in this polymer in polar β-modification.[22] It is known that for the latter the conformation of plain zigzag is typical, with dipolar moment perpendicular to the macromolecular axis, while the chains in α-phase have $TGTG^-$ conformation, which have nonzero component of the dipole moment $\mu_{||}$ directed along the chain axis.[8] The axes are oriented practically perfectly along the drawing axis in textured PVDF films with α-phase macromolecular crystals. In these films, if the external electric field is applied along and then across the drawing axis, the contribution of $\mu_{||}$ to the mechanism of α_c-relaxation can be revealed. Such experiments have been described in Ref. 14. The result is that dielectric strength of α_c-relaxation in those highly anisotropic films was found to be maximal when the directions of the drawing axis and the applied electric field were the same, while reduced to zero when perpendicular. It was proposed that α_c-transition is related to reversible conformational rearrangements $TGTG^- \leftrightarrow G^-TGT$ in the crystal, at which $\mu_{||}$ changes its direction to the opposite. The character of changes in intensity of 120 and 031 peaks in the region of α_c-process is in the agreement with such conclusion.[38] On the other hand, other authors propose totally different mechanism for this transition in PVDF. For example, the transition around 40°C (in the temperature region of α_c-process)[12] is attributed to the upper glass transition point (T_g^U), i.e., to the relaxation in RAP, as it is observed in other crystalline polymers.[43–45]

EXPERIMENTAL

VDF/HFP copolymers of 93/7 and 86/14 ratios have been studied in this paper. Their chain microstructure was earlier characterized by high resolution NMR.[46] The films were prepared by the method of extrusion by squeezing the melt through the slit head. X-ray data show that *c*-axis of crystals are weakly oriented in relation to the extrusion axis. After the preparation, the films were stored at room temperature for several years. Thickness of the films was 64 μm. For electrical measurements, 0.1-μm thick Al electrode was evaporated in vacuum.

Novocontrol setup was used to study dielectric properties of the copolymer films in isothermal regime at frequencies 10^{-1} to 10^7 Hz and in the temperature range −100 to 150°C. Differential scanning calorimetry (DSC) experiments were carried out using the Perkin-Elmer DSK-7. Heating range of 20 mg samples was 20°/min. Calibration was made by In. Wide angle X-ray diffraction (WAXS) data at 0.154 nm wavelength was obtained using the Kard-6 type setup with two-dimensional position-sensitive detector made in Institute of Crystallography RAS.[47] Measurement was performed in transmission mode. Separation of overlapping reflexes was made with the help of standard program using different functions for description of a line profile.

RESULTS AND DISCUSSION

Figure 1 shows three-dimensional representation of the dielectric loss tangent as a function of temperature and log(frequency) for VDF/HFP 93/7 (a) and 86/14 (b) films. Three or four relaxation processes, depending on the composition of the copolymer, are clearly observed. Later we will accent on the question how HFP comonomer concentration changes the parameters of the relaxations. In this connection, it is useful to analyze the structure of copolymers with different comonomer concentrations. DSC scans [Fig. 2(a,b)] show that at heating above room temperatures, there is different amount of transitions accompanied by calorific effect. For 14 mol % HFP there are two of them evidently observed, and for 7 mol % there are three. To clarify this result, WAXS difractograms are presented in Figures 3–5 for PVDF and both copolymers.[47] It is seen from Figure 3 that PVDF crystallizes in α-phase. As seen from Figures 4 and 5 the copolymers crystallize in the same phase (as showed in papers[48,49]) but with lower perfection. On increase of HFP content the number of peaks typical for this phase and their intensity decrease, which leads to the decrease of crystallinity ϕ. $\phi = 0.48$ in PVDF,[47] while it is equal to 0.21 for VDF/HFP 93/7 copolymer and decreases to 0.17 for 86/14 copolymer. Qualitatively the same tendency was mentioned for similar copoly-

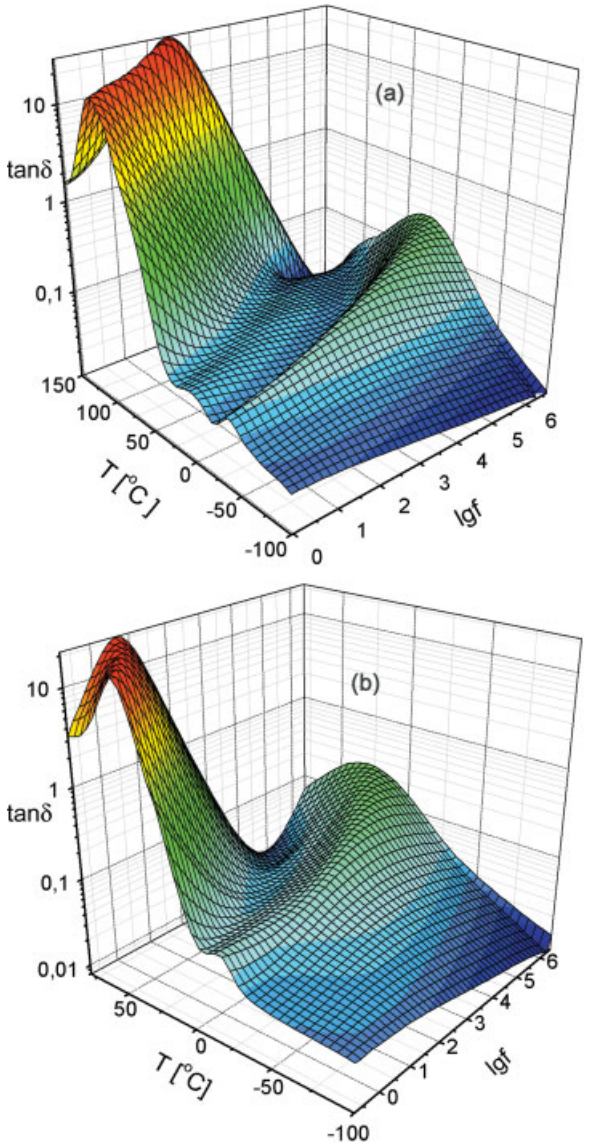

Figure 1 3D representation of the tanδ frequency and temperature spectrum for VDF/HFP 93/7 (a) and 86/14 (b) copolymers. [Color figure can be viewed in the online issue, which is available at www.interscience.wiley.com.]

mers in Refs. 50 and 51. Besides, from Figures 3–5 it is seen that the peaks are essentially broader if the HFP fraction is higher. It means that the crystal size decrease along different crystallographic directions. This fact can cause lowering of melting point of forming crystals when HFP content increases from 7 to 14 mol % [Fig. 2(a,b)]. Similar behavior was mentioned in Ref. 51.

We will consider mechanisms of differences in relaxation processes in polymers under study taking into account these structural data. In Figure 6(a,b) frequency dependencies of dielectric loss factor ε″ for the temperatures below room are shown for both copolymers. In both copolymers a relaxation process is detected at temperatures lower than −40°C (designated here as β-) with very broad distribution of relaxation times. By analogy with homopolymer, it is attributed to the local mobility of VDF chains.

The analysis shows that as in other polymer systems[52] experimental curves in Figure 6 are generally described by function

$$\varepsilon^*(\omega) - \varepsilon_\infty = \sum_k \frac{\Delta\varepsilon_k}{\left[1 + (i\omega\tau_k)^{1-a_k}\right]^{b_k}} - iA\omega^{-s} \qquad (1)$$

Here the empirical Havriliak–Negami function (first term) describes relaxation mobility of bound charges, and the second term is for the relaxation of mobile charges. Here $\Delta\varepsilon = \varepsilon_0 - \varepsilon_\infty$ is the relaxation strength (ε_0 and ε_∞ are the low- and high-frequency limits of the real part of dielectric permittivity ε'), $\omega = 2\pi f$ is the angular frequency of the electric field, a and b ($0 \leq a, b \leq 1$) are parameters describing asymmetry and width of distribution of relaxation times respectively, τ is the relaxation time, A is the constant, $s \leq 1$ is the exponential factor.[53]

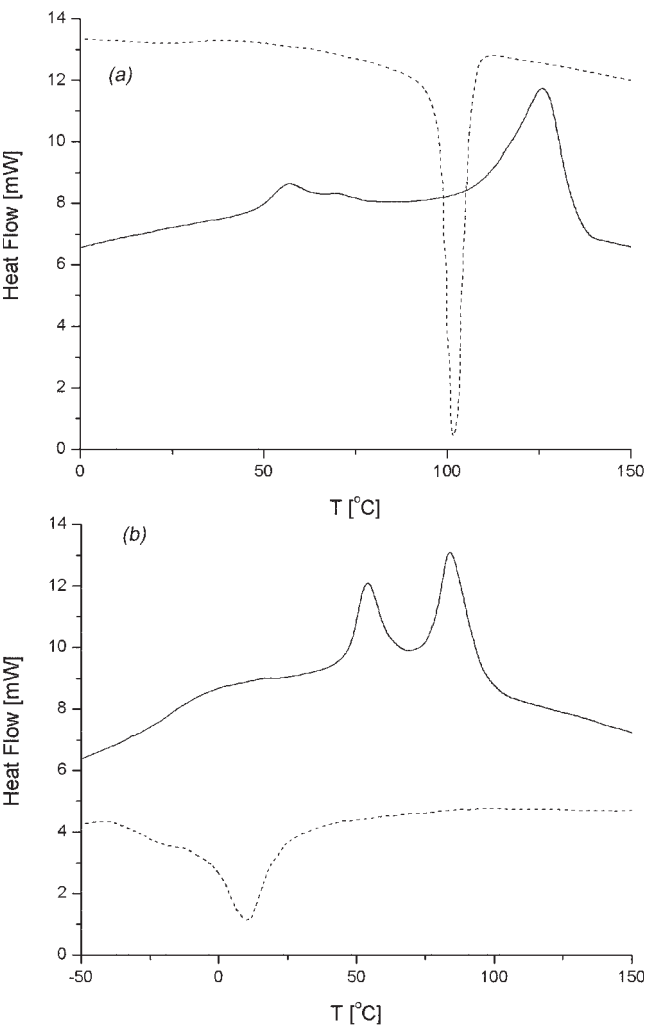

Figure 2 DSC thermograms for the first heating (solid lines) and cooling (dashed lines) cycle for VDF/HFP 93/7 (a) and 86/14 (b) copolymers.

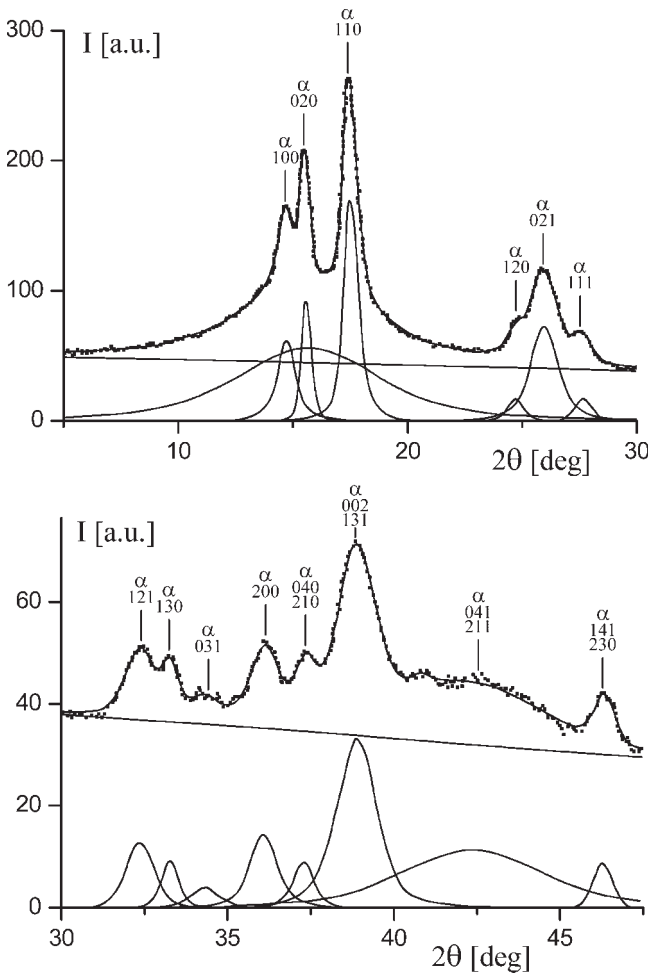

Figure 3 Wide angle X-ray diffraction for isotropic PVDF film obtained by isothermal crystallization from the melt.

The example of dielectric loss spectra decomposition according to eq. (1) is presented in Figure 7. At given temperatures the 86/14 copolymer is characterized by one relaxation process (α_a- in our terminology). For the 93/7 copolymer there are two processes. They are more clearly separated at temperature dependencies of ε' and tanδ at $f = 1.3$ kHz (Fig. 8). For both copolymers two relaxation processes (α_a- and β-) at low temperatures are seen. The local β- process manifest itself as a low-temperature asymmetry on the α_a-intensive peak on tan(T) curve. There is an additional dispersion region near 50°C for the copolymer with 7 mol % HFP. At Figure 9 $\varepsilon''(T)$ curves are presented for both samples in this temperature region. According to the Figure 9(a), it has a relaxation character. This process is not observed in the copolymer with higher amount of HFP [Fig. 9(b)]. As long as temperature position of this type of mobility is the same in PVDF[8] crystallized in the same phase, we designated it as α_c-process.

Let us consider the reasons why there is no such process in the VDF/HFP 86/14 copolymer. As mentioned earlier, its crystallinity is lower than that for the copolymer with 7 mol % HFP. It means that the noted process is related to the crystalline phase. The most generally accepted mechanism for the α_c-transition in PVDF crystals with nonpolar lattice is reorientation of dipole moment's longitudinal component $\mu_{||}$ for the chain fragment in the TGTG$^-$ confirmation. Molecular mechanism of such reorientation assumes movement of the conformational defect along the crystal c-axis.[39] It can be realized as solitone waves.[54,55] It means that crystal dimension along this axis must affect on the α_c-transition characteristics. As follows from comparison of Figures 4 and 5, increase in HFP amount leads to broadening of 002 peak, which characterizes longitudinal (along the macromolecular axis) crystal dimension. It decreases from 2.9 to 1.4 nm.[47] Double decrease in longitudinal dimension of crystals in α-phase and decrease in its volume fraction can account for the absence of the α_c-dispersion in VDF/HFP 86/14 copolymer films. Calorimetric data do not clarify the mechanism of this process. Indeed, there is one more endothermic transition at ($\sim$ 70°C besides the melting peak in PVDF samples

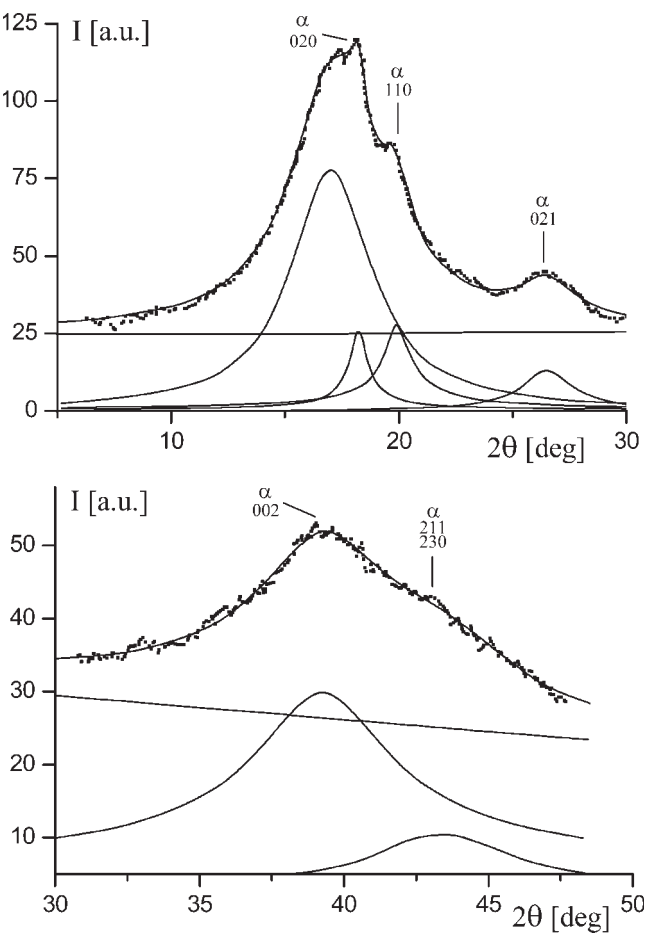

Figure 4 Wide angle X-ray diffraction for initial VDF/HFP 86/14 film.

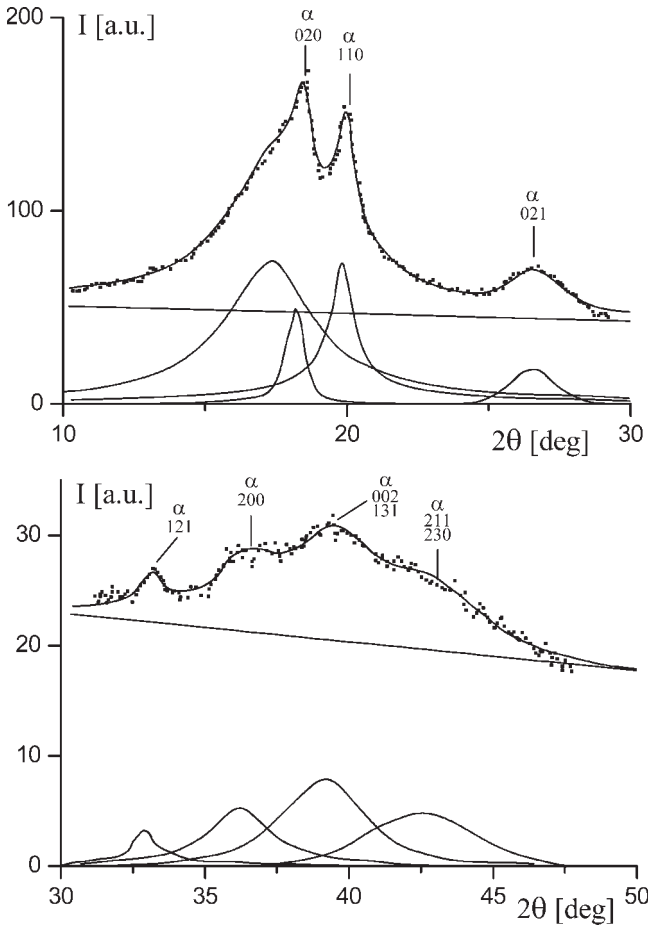

Figure 5 Wide angle X-ray diffraction for initial VDF/HFP 93/7 film.

with α-modification prepared by nonisothermal crystallization by quenching from the melt. This mechanism disappears at annealing[56–58] (or after repeated heating cycle[57]). The authors[56,58] consider it as an indication for the existence of upper glass transition point (T_g^U), where RAP relaxation occurs.[12,43–45] The authors[57] do not agree with this. On their opinion, this relaxation process is connected with the transition of ordered regions into the condis-crystal state, and its molecular mechanism is suggested.[14,38]

Calorimetric data in considered temperature range also reveal multiple thermal peaks for our copolymers (Fig. 2). Three peaks are observed in VDF/HFP copolymer with 7 mol % of HFP [Fig. 2(a)], whereas when HFP fraction goes up to 14 mol % their number decreases to two [Fig. 2(b)]. It has to be emphasized that the latter effect is reproductable, because it is registered in films of different thickness and after reducing of the heating rate by order of magnitude. As it will be shown later, the low-temperature endothermic transition in Figure 2(b) for VDF/HFP 86/14 copolymer and the second peak (around 70°C) in the copolymer with 7 mol % HFP are connected with ferroelectric phase transition. From comparison of Figures 8(a) and 9(a) it is seen that in the region of α_c-relaxation, endothermic transition [low-temperature peak at ~ 60°C in Fig. 2(b)] appears in VDF/HFP 93/7 copolymer. Therefore, there is a correlation between the appearance of α_c-relaxation in the polymer and the existence of additional thermal peak in this region. These data do not completely exclude that the transition is connected with the relaxation of the rigid amorphous phase. It can be supposed that the fact that crystallinity in the VDF/HFP 93/7 copolymer increases (also due to the increase in crystals sizes, as mentioned earlier) the appearance of the rigid amorphous phase, which manifests itself in the observed α_c-relaxation, is more possible.

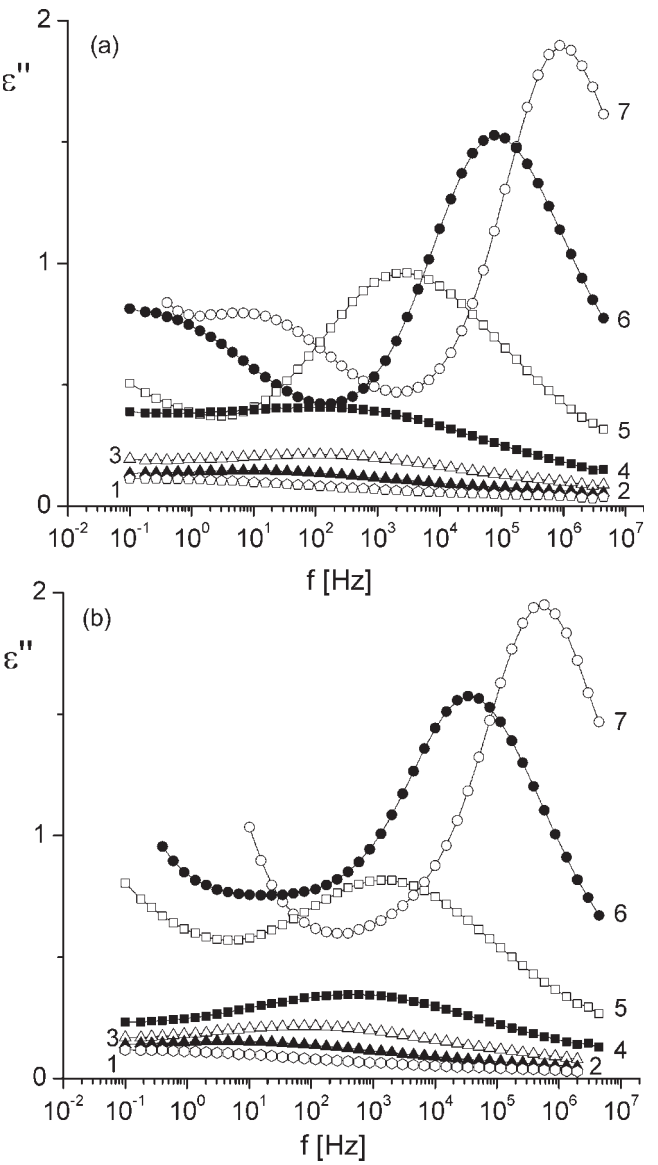

Figure 6 Frequency dependencies of the dielectric loss ε″ in initial VDF/HFP 93/7 (a) and 86/14 (b) copolymer films at (1) −100°C, (2) −80°C, (3) −60°C, (4) −40°C, (5) −20°C, (6) 0°C, and (7) 20°C.

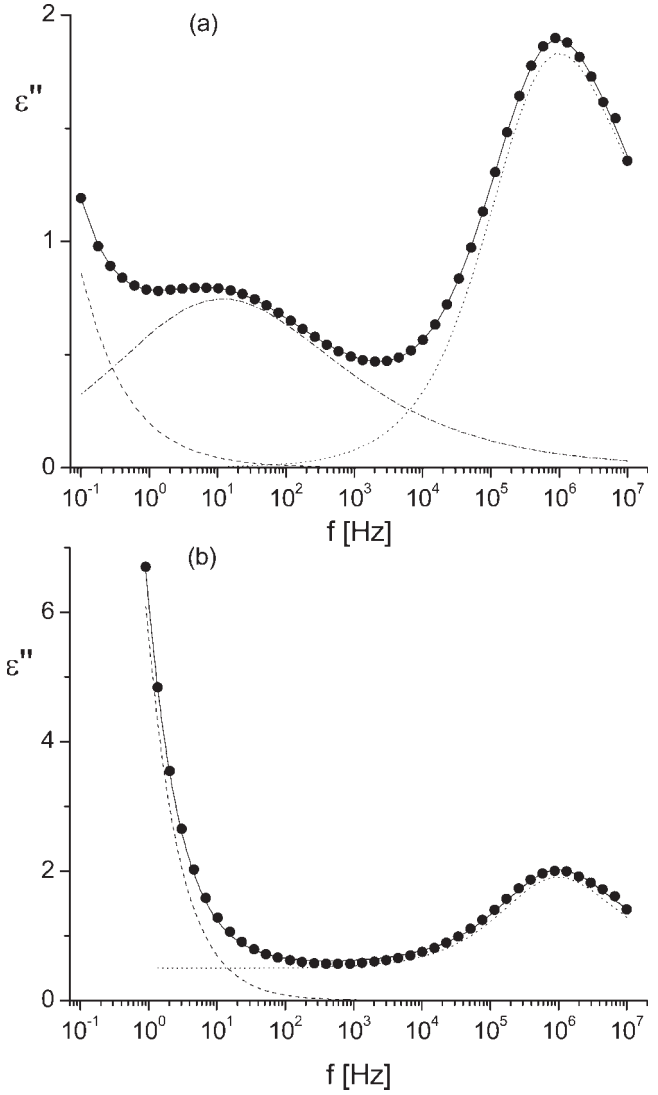

Figure 7 Example of decomposition of the dielectric loss ε'' spectra for VDF/HFP 93/7 (a) and 86/14 (b) films at 25°C.

Temperature behavior of the relaxation transitions mentioned earlier has been characterized by means of the correlation diagram in Arrhenius coordinates (Fig. 10). It is seen that the lowest-temperature (β-) transition obeys the Arrhenius equation

$$f = f_0 \exp\left(\frac{-\Delta E}{RT}\right), \tag{2}$$

where f_0 is the constant, R is the gas constant, ΔE is the activation energy, and T is the temperature. According to this figure and to the data presented in Table I, characteristics of this transition practically do not depend on the composition of the copolymer. The same conclusion for the copolymers under study was drawn from the mechanical relaxation.[59,60] As seen from Figure 10, α_a-processes that are registered at higher temperatures (curves 2,2′) do not obey eq. (2), but are described by the Vogel–Thamman–Fulcher equation

$$f = f_0 \exp\left(\frac{-B}{T - T_0}\right), \tag{3}$$

where f_0 and B are fitting parameters, T_0 is the characteristic temperature, which is usually ~ 50°C lower than the T_g. It is known that such behavior is typical for the microbrownian motions in the amorphous phase at glass transition. The values of indicated parameters are presented in Table I. At the same time the conventional glass transition temperature T', for which the frequency of reorientation of the kinetic units is 1 Hz, was determined from curves 2,2′. It follows from Table I that when HFP fraction increases, T' also increases. It was also mentioned earlier.[50,51,59,61] Since the glass transition temperatures of both components of the copolymers differ in more than 200°, the noted behavior is predicted by the modified Fox equation[61]

$$1/T_g = \sum_{i,j} W_i P_{i,j} / T_{g_{i,j}}. \tag{4}$$

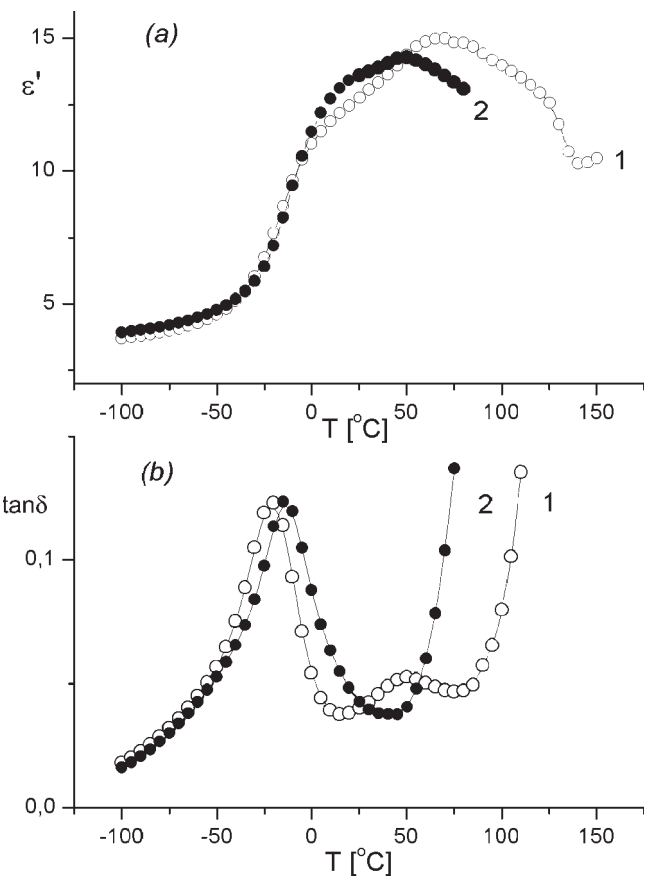

Figure 8 Temperature dependencies of the dielectric permittivity ε′ (a) and the tanδ (b) for initial 93/7 (1) and 86/14 (2) copolymers at $f = 1300$ Hz.

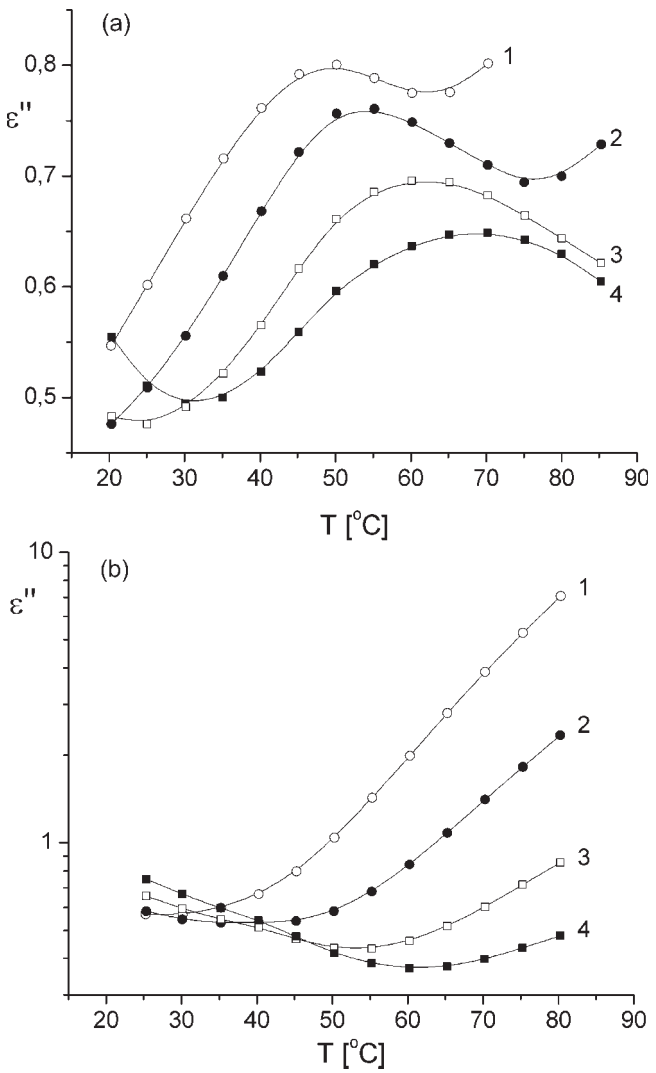

Figure 9 Temperature dependencies of the dielectric loss ε″ for VDF/HFP 93/7 (a) and 86/14 (b) films in the region of α_C-relaxation at (1) 390 Hz, (2) 1300 Hz, (3) 4500 Hz, and (4) 10^4 Hz.

Here W_i is the weight fraction of the i-th component of the copolymer with the glass transition temperature $T_{g_{i,j}}$, $P_{i,j}$ is the factor determining the appearance of dyads, triads, etc. in chains, registered by the NMR method in copolymers.[61] Such prediction is qualitative, because the noted equation is rigorously true for noncrystallizing polymers. Our polymers are crystalline, and therefore two factors will affect the glass transition point. On the one hand, it is the weight ratio of HFP comonomer, and on the other hand it is the change in the copolymer crystallinity. According to eq. (4), as the HFP content changes from 7 to 14 mol %, the T_g must increase. From the other hand, as mentioned before, crystallinity decreases almost in two times. It is known that the rigid wall of the crystal is the topological barrier for the microbrownian motion in the amorphous phase. Therefore, the increase in crystallinity usually results in the increase of the relaxation time for the α_a-transition[62–64] and of the glass transition temperature.[45] Moreover, for the copolymer with higher HFP content the dimensions of the amorphous space between adjacent lamellae packed into stacks increase from 7.6 to 14.6 nm.[47] By the example of isotactic polystyrene it was shown that this must lead to the decrease of relaxation time of the transition under consideration.[65] From this point of view, the increase of HFP content from 7 to 14 mol % must cause, other things being equal, the decrease of the glass transition point, i.e., opposite to the eq. (4). In this connection, all the factors listed earlier will take effect on the temperature position of the α_a-transition relaxation times when HFP content increases.

Curves 2 and 2′ in Figure 10 have different curvature. It specifies that the glass transition processes in both copolymers differ by the thermodynamic parameter fragility m, which in terms of VFT equation can be calculated according to the relation

$$m = \frac{d\log\tau}{d\left(\frac{T'}{T}\right)} = \frac{B}{T'\ \ln 10\left(1-\frac{T_0}{T'}\right)^2}. \tag{5}$$

Here τ has the same sense as in eq. (1). The values of the parameter m are listed in the Table I. It is higher for the copolymer with 14 mol % of HFP. This can be ascribed to the increase in number of groups with sterical hindrance and to the increase of the amorphous phase content, where this relaxation occurs.

Temperature dependencies of β- and α_a-relaxation parameters, which were obtained after decomposition of overlapping processes according to eq. (1), are presented in Figure 11. The character of showed curves essentially changes in the transition region from the local mobility in the glass state to the segmental mobility above the glass transition point. Thus, it is seen that the spectrum narrows ($b \to 1$) and become more symmetric ($(1 - a)$ increases). Some notes are to be made about the character of temperature changes of the relaxation strength Δε. As seen from the Figure 11(c), it also changes essentially in the glass transition region. Week increase of Δε in glassy state noticeably intensifies at temperatures above the glass transition point (~ -40°C). This behavior is not trivial and needs to be explained. Such problem is discussed with reference to other crystalline polymers.[43–45] It is known that

$$\Delta\varepsilon \approx \frac{N\mu_e^2}{kT}, \tag{6}$$

where N and μ_e are the concentration and the effective dipole moment of kinetic units in the amorphous phase. For the relaxation process in crystalline polymers it is convenient to introduce the parameter.[43]

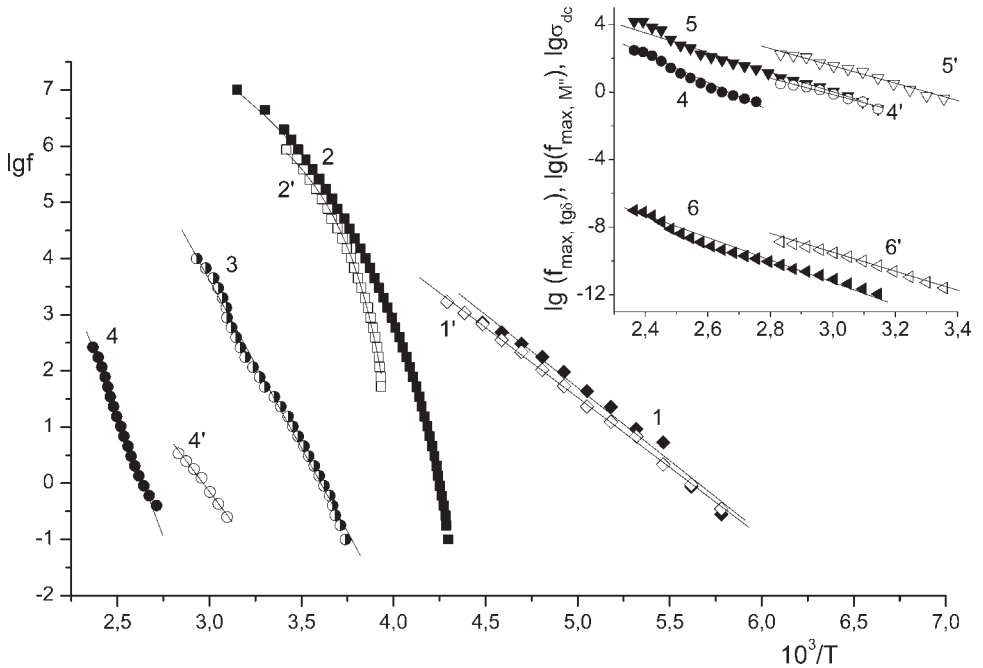

Figure 10 Correlation diagrams for relaxations in VDF/HFP 93/7 (1–6) and 86/14 (1′, 2′, 4′-6′) copolymers: 1,1′ – β-relaxation; 2,2′ – α_a-relaxation; 3 – α_c-relaxation; 4,4′ – α-relaxation. Curves 1–3, 1′,2′ are obtained from the tanδ(T) dependencies, 4,4′ – from the tanδ(f) dependencies. On the insert Arrhenius plots are shown for the loss tangent tanδ (4,4′), the imaginary part of electric modulus M'' (5,5′) and the dc-conductivity σ_{dc} (6,6′) in the region of the α-relaxation.

$$\beta(T) = \frac{\Delta\varepsilon(T)^{sc}}{\Delta\varepsilon(T)^{a}}, \tag{7}$$

which has the sense of the relaxed amorphous phase content, where sc and a indices are for partly crystallized and amorphous polymer. For some polymers, which can be obtained in the amorphous and crystalline states, $\Delta\varepsilon(T)^a$ and $\Delta\varepsilon(T)^{sc}$ dependencies exhibit opposite temperature behavior. For example, for the amorphous polymers (polyether etherketon[43] or polyphenylenesulphide[44]) Δε decreases with temperature for this process. If the numerator is constant, this decrease is qualitatively predicted by Ref. 6. On the other hand, if the mentioned polymers are crystalline, $\Delta\varepsilon(T)$ must increase[43,44] for the α_a-process. The last condition is ascribed to the relaxation of the rigid amorphous phase RAP, which can be localized on the crystal–amorphous phase boundaries. According to the temperature data of the specific heat, RAP formation is usually observed in semirigid polymers.[43–45] On the other hand, in flexible polymers (PE, PTFE) of the rigid amorphous phase is not formed.[66,67]

The investigated polymers are flexible also and therefore the RAP is not formed.[57] On the other hand, our data on temperature dependence of Δε in the region of α_a-relaxation [Fig. 11(c)] are typical for polymers with RAP relaxation. In this connection, there is a quite nontrivial conclusion. According to the dielectric method, elastomeric materials (especially it concerns VDF/HFP 86/14 copolymer with low degree of crystallinity), exhibit behavior that is typical for RAP relaxation in the region of segmental α_a-mobility. This behavior formally corresponds to very wide and diffuse glass transition area. DSC data [Fig. 2(b)] indicate it also. In the investigated polymers, there are groups with large dipole moment in the main chain. They cause ferroelectricity.[1,2,4] Thus, in these copolymers spontaneous polarization regions (nanometer in size) can be formed. If those are present here (we shall consider some indications on it further), then, together

TABLE I
Parameters of Vogel–Thamman–Fulcher Analysis [eq (3)]

Relaxation process	Composition						
	93/7				86/14		
	β	α_a	α_c	α	β	α_a	α
T_0 (K)	–	199	–	–	–	233	–
B	–	845	–	–	–	305	–
a	–	10	–	–	–	8	–
ΔH (kJ/mol)	47	78	112	151	47	97	81
ΔS (J/mol K)	40	–	173	168	37	–	5
T' (K)	177	235	278	379	179	255	341
m	–	65	–	–	–	70	–
C_1		2,970				6,060	
C_2		4,050				3,990	

ΔH, enthalpy; ΔS, enthropy; T', conventional glass transition temperature; m, fragility; and C_1 and C_2, Curie constants for relaxation processes in VDF/HFP copolymers of different composition.

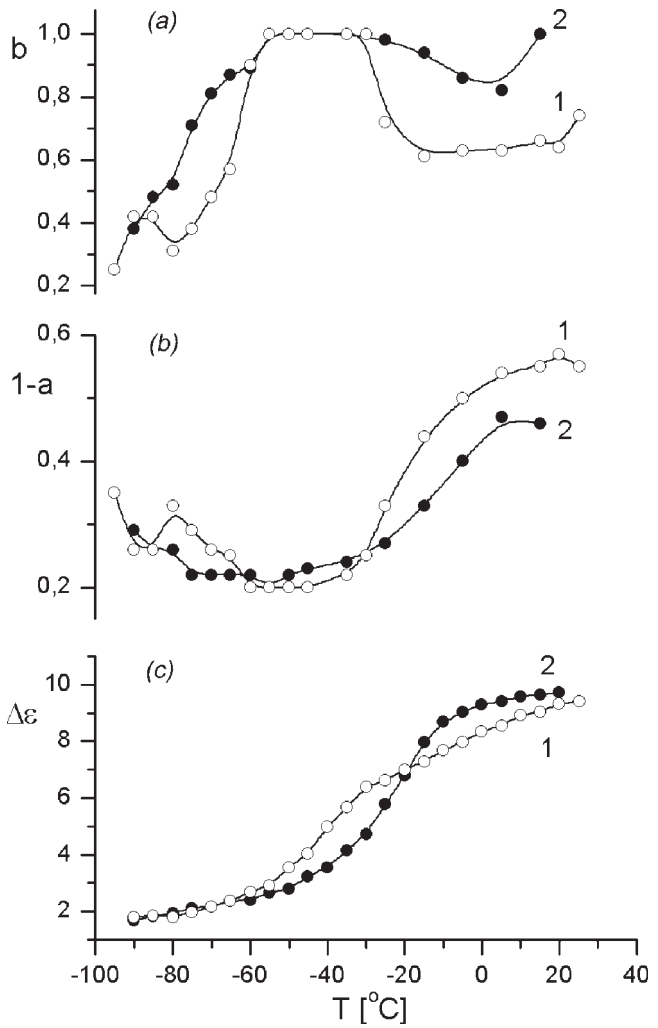

Figure 11 Temperature dependencies of the spectrum width (a), the asymmetry (b), and the relaxation strength (c) in the region of β- and α_a-transitions in VDF/HFP 93/7 (1) and 86/14 (2) copolymers.

with small crystals of α-phase, they can play a role of labile physical crosslinks. Segments of the amorphous phase above the glass transition can partially lose mobility near these crosslinks and show some properties of RAP. If the number of assumed nanocrystals is great enough, all amorphous phase can be considered as an interphase and show properties of RAP. Such model can explain mechanisms of considered α_a-relaxation in our copolymers. On the other hand, such assumption agrees with conclusion of authors,[28,29] on which the relaxation above the glass transition point in the given class of polymers is due to the mobility of the amorphous segments in the interphase.

To confirm the introduced model let us stop on basing of presence of assumed spontaneous polarization areas of nanometer size in amorphous phase in more detail. If such areas exist, there should be a ferroelectric–paraelectric type transition in them (as well as in usual ferroelectric crystals). It is registered by thermal or electric anomalies. VDF/HFP 86/14 copolymer is the most convenient object, because above the room temperature there is no α_c-process, which can mask mentioned anomalies. From Figure 2(b) it is seen that there are two endothermic transitions at the first heating cycle in the initial sample of this copolymer above room temperature. Transition at highest temperature is connected to melting of α-phase crystals. At lower temperatures (around $\sim 50^\circ$C), there is a clearly recognized peak that is also registered on similar 85/15 copolymer.[48] To our opinion, this peak is responsible for the mentioned ferroelectric–paraelectric transition in supposed nanometer areas of spontaneous polarization.

If such hypothesis is true, one also can expect dielectric permittivity anomalies in this region. They are well-defined for the copolymer with 14 mol % HFP [curve 2 in Fig. 8(a)]. It is seen that the diffuse peak of ε' and the first endothermic transition are in the same temperature region. The registered transitions are more complex for VDF/HFP 93/7 copolymer. As noted earlier, α_c-transition is also registered in considered temperature region. This transition is accompanied by absorption of heat [low-temperature endothermic peak at heating in Fig. 2(a)]. The peak at higher temperatures, in our opinion, is responsible for mentioned ferroelectric–paraelectric transition. As follows from Figure 8(a), the peak of the dielectric permittivity for this copolymer (curve 1) is in this temperature region. Temperature dependencies of dielectric permittivity in wide temperature range [Fig. 8(a)] are like those for a classical ferroelectric polymer–copolymer of VDF and trifluorethylene TrFE of 65/35 ratio.[31] Differences are that for the latter the peak on $\varepsilon'(T)$ curve in the Curie point is more intensive.

Use of classical representations of such transitions by temperature dependencies of reciprocal dielectric permittivity $\chi = 1/\varepsilon'$ can serve as additional argument to ascribe the considered process to a ferroelectric–paraelectric phase transition. In Figure 12 they are shown for both copolymers. At a variation of frequency of the electric field on two decades the position of a temperature minimum (T_t) practically does not change, that is typical for phase transitions of considered type. Regular change of minimum magnitude with change of frequency of the electric field, along with its high diffuseness, speak in favor of relaxor type[68] of the transition. It is also known that considered dependencies straighten near the transition temperature (T_t) and thus follow

$$\chi \sim \frac{(T_t - T)}{C_1} \quad \text{at} \quad T < T_t \quad \text{and} \quad \chi \sim \frac{(T - T_t)}{C_2} \quad \text{at } T > T_t \qquad (8)$$

Constants C_1 and C_2 calculated for both copolymers are presented in Table I. Comparison with data on the

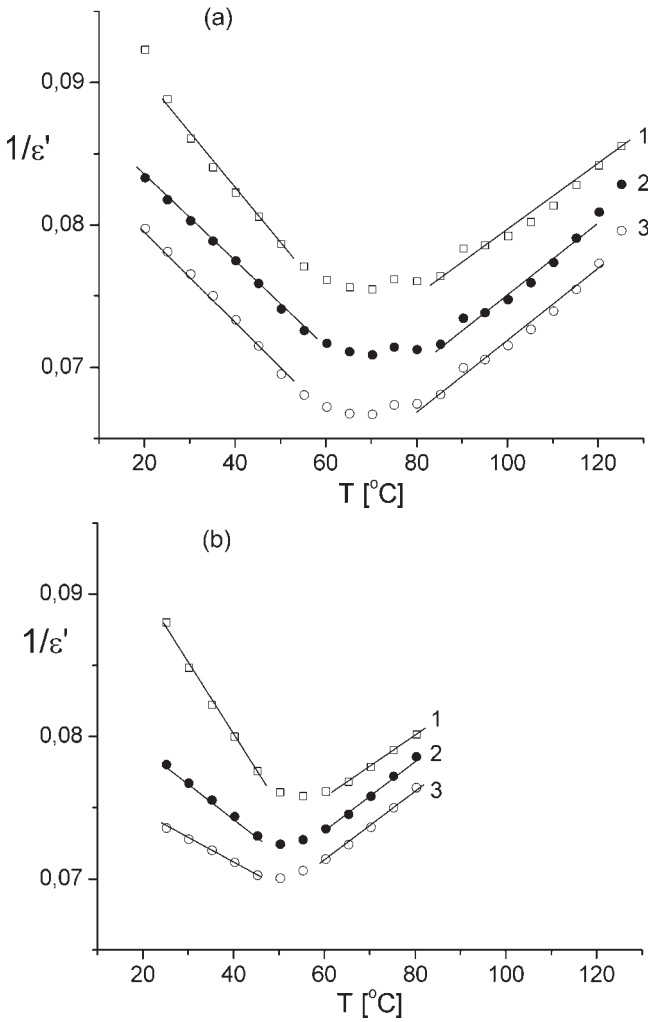

Figure 12 Temperature dependencies of the dielectric susceptibility χ in 93/7 (a) and 86/14 (b) copolymers at f = 120 kHz (1), 10 kHz (2), 1.3 kHz (3).

Curie transition, for example, in VDF/TrFE 52.8/47.2 copolymer[24] shows that C_2 is of the same order. It follows from Figure 12 that when HFP content increases from 7 to 14 mol %, phase transition shifts by 20° to lower temperatures and becomes more diffuse (compare C_1 in Table I). If such transition is attributed to manifestation of dipole interactions, then it is obviously caused by their weakening due to the increase of nonpolar HFP group's concentration in chain. Such assumption is confirmed also by data in Ref. 69 where ferroelectric properties of VDF/TrFE/HFP terpolymers are investigated. By results of calorimetric and dielectric investigations, it has been shown that the increase of HFP ratio is also accompanied by widening of the Curie transition with its simultaneous shift to lower temperatures.

As our copolymers crystallize in nonpolar α-phase with zero spontaneous polarization, there are no areas of spontaneous polarization connected with polar β-modification.[2,4] Thus, the data presented earlier point out that one more ferroelectric phase possibly develop in our objects. The question of presence of two types of ferroelectric phase for this class of polymers is not new and is often discussed by different authors.[2] The facts of occurrence of two dielectric anomalies in copolymers VDF/TrFE 70/30 or specific shape of ferroelectric switching curves[70] are usually used as arguments. These two phases are designated as LT and QL in terminology of Ref. 71. Low-perfect QL-phase is characterized by presence of a great number of conformational defects. It is possible that transition of this phase into a paraelectric state is registered in our copolymers. We can consider that small regions of spontaneous polarization of QL-phase are localized in the amorphous areas. A number of facts speak for it. The heat of considered transition in VDF/HFP 86/14 copolymer is 4 J/g, while in a 7 mol % HFP copolymer it is 1.1 J/g. If the mentioned domains are localized in the amorphous phase, heat of transition, with other things being equal, will be defined by its volume fraction. As noted earlier, its fraction is higher in a copolymer with 14 mol % HFP. It supports the hypothesis about the localization of spontaneous polarization domains in the amorphous phase. Thus the domain size can be estimated by the width of the amorphous halo.

It was noted above that ferroelectric transition temperature falls 20° lower when HFP content increases from 7 to 14 mol %. If noted transition occurs in domains of the amorphous phase, its microstructure should change. We shall speak about average density of packing of segments in such phase. To a first approximation it is possible to judge about it by angular position of the amorphous halo. The analysis of data in Figures 4 and 5 shows that the increase in HFP ratio leads to shift of noted angular position 2θ to lower degrees,[72] and the same tendency was also noted earlier.[50] It points to the fact that when HFP content increases from 7 up to 14 mol %, average interchain distances in the amorphous phase of the copolymer essentially rise. Thus, lowering of ferroelectric transition temperature in the copolymer with high HFP content correlates with reduction of packing density in its disordered phase. This can also lead to more diffusive phase transition (see C_1 values in Table I).

Recent data on dielectric properties of PVDF films prepared by thermal vacuum deposition[73] support the hypothesis about localization of discussed spontaneous polarization domains in the amorphous phase. According to these data, order–disorder ferroelectric transition of relaxor type was observed in amorphous PVDF[73] at the same temperatures.

Now let us discuss how much reasonable it is to speak about spontaneous polarization areas in the disorder phase? The analysis of literary data shows that such assumptions are physically proved. Really, the

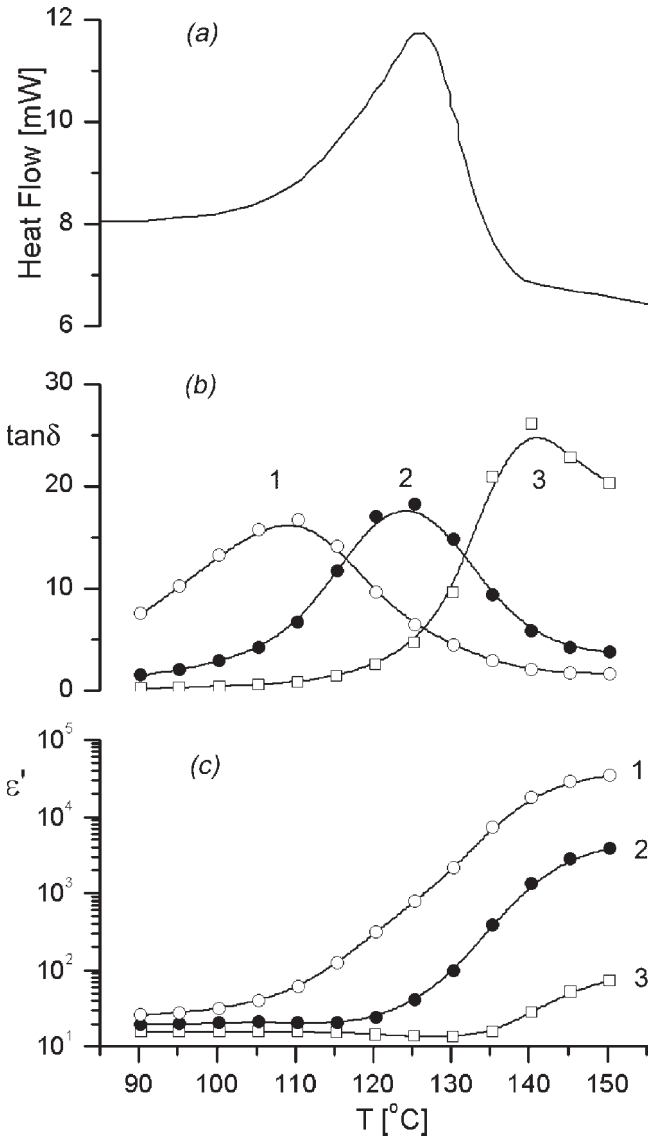

Figure 13 Temperature dependencies of the heat flow (a), the tanδ (b), and dielectric loss ε″ (c) in the region of α-relaxation in VDF/HFP 93/7 copolymer at $f = 1.3$ Hz (1), 10 Hz (2), and 120 Hz (3).

ferroelectric behavior is noted both in organic[74] and in classical inorganic[75] glassy dielectrics with disordered structure. Specificity of formed structure in our copolymers can be determined by means of preparation of initial films. As noted earlier, they were prepared by extrusion. In this case, the surface can be more textured than the volume, and the discussed spontaneous polarization areas can be localized in surface layer. Therefore, the annealing effects should affect both the structure characteristics and the parameters of discussed ferroelectric transition. We have got preliminary evidence on it earlier,[46] and now we clarify stated assumptions by structural methods.

Next, we shall discuss the nature of high-temperature α-relaxation process observed in both copolymers. It is characterized by extremely high intensity, as seen in Figure 1. Some details of noted transition follow from Figure 13. Here temperature dependencies of exothermal heating at crystals' melting and tanδ for the region of considered relaxation process are shown for VDF/HFP 93/7. At melting free volume varies and the geometry of the measured condenser can change, and so we characterized dielectric parameters by dielectric loss tangent. It allows to exclude a role of possible change in geometry of measured condenser. It is seen from the figure that tanδ peak at low frequencies falls at the region of melting temperatures. Similar behavior was noted for VDF/HFP 86/14 copolymer (Fig. 14). It means that appearing of α-relaxation process is initiated by the process of crystals' melting. We shall consider three possible reasons. If the crystal transitions into the melt, then the chains can move as a whole; that leads

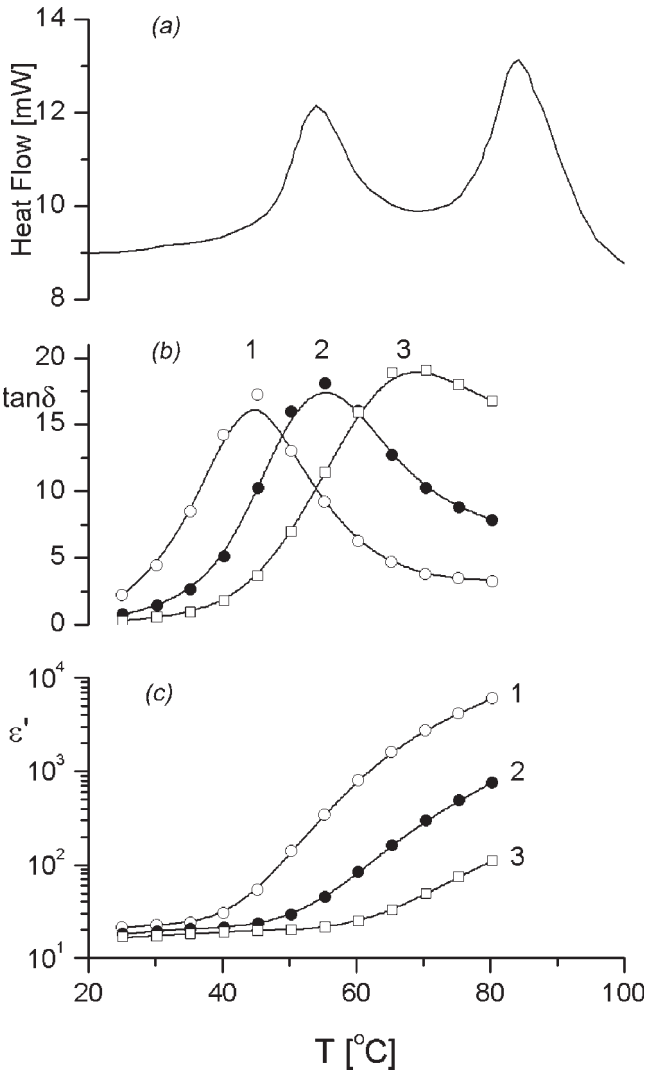

Figure 14 Temperature dependencies of the heat flow (a), tanδ (b) and dielectric loss ε″ (c) in the region of α-relaxation in VDF/HFP 86/14 copolymer at $f = 0.1$ Hz (1), 0.4 Hz (2), and 1 Hz (3).

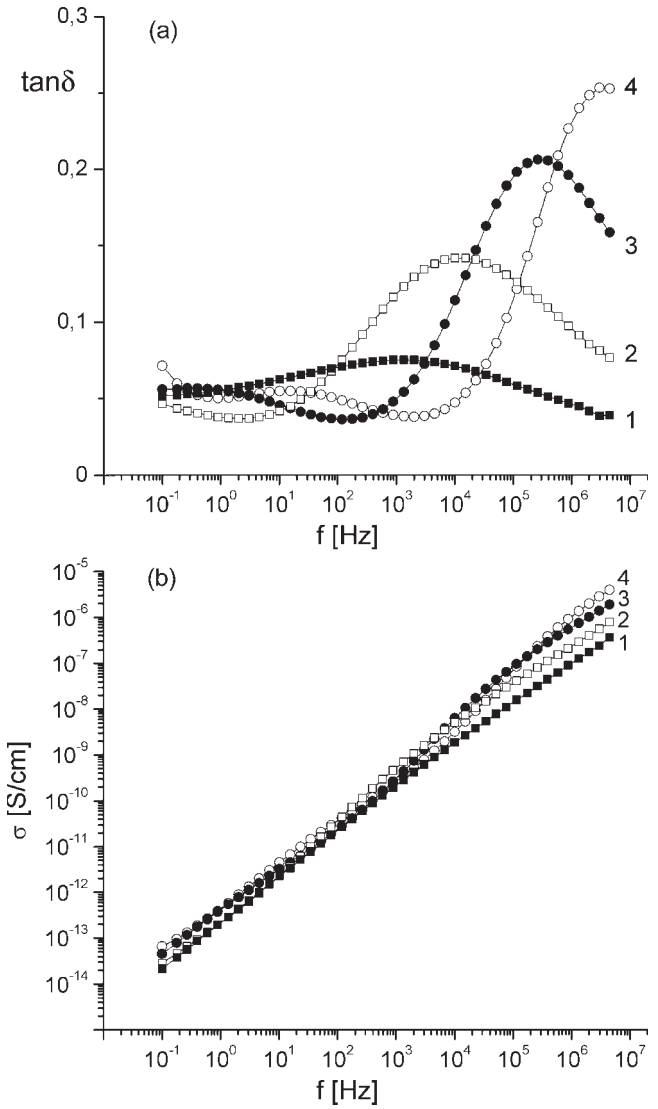

Figure 15 Frequency dependencies of the tanδ (a) and conductivity σ (b) in the region of α_a- and α_c-relaxations for VDF/HFP 93/7 copolymer at (1) −40°C, (2) −20°C, (3) 0°C, (4) 20°C.

to occurrence of fluctuations of distance between chain ends. In this case, under certain conditions, normal mode relaxation appears.[76–78] The relaxation strength Δε for the given type of mobility[76]

$$\Delta\varepsilon = \frac{4\pi\mu_u^2\langle r^2\rangle N_A\rho}{3k_BTM}F. \quad (9)$$

Here N_A is the Avogadro number, M is the molecular weight, ρ is the density, μ_u is the dipole moment of the unit of countor length, $\langle r^2\rangle$ is the root-mean-square distance between the chain ends, F is the internal field factor which for a normal mode relaxation is close to 1. According to eq. (9) given process will be observed if the longitudinal component of the dipole moment is present. It is not zero for our copolymers, which are crystallized in α-phase with TGTG$^-$ chain conformation. It is also correct for the melt that contains noncorrelated TG and TG$^-$ sequences.[4] Because of this, such relaxation process should be present in considered copolymers. To connect observable α-process with a normal relaxation mode it is necessary to investigate characteristics of the given process in copolymers with various monodisperse fractions, as parameters of this relaxation appear to depend strongly on polymer molecular weight.[77,78]

The second mechanism of α-relaxation must take account of heterogeneous nature of crystalline polymers. Crystal and amorphous phases are of different symmetry. Above the glass transition point and below the melting temperature there is not only structural heterogeneity, but heterogeneity of dynamic characteristics also. This is because the amorphous phase segments (contrary to crystal) participate in

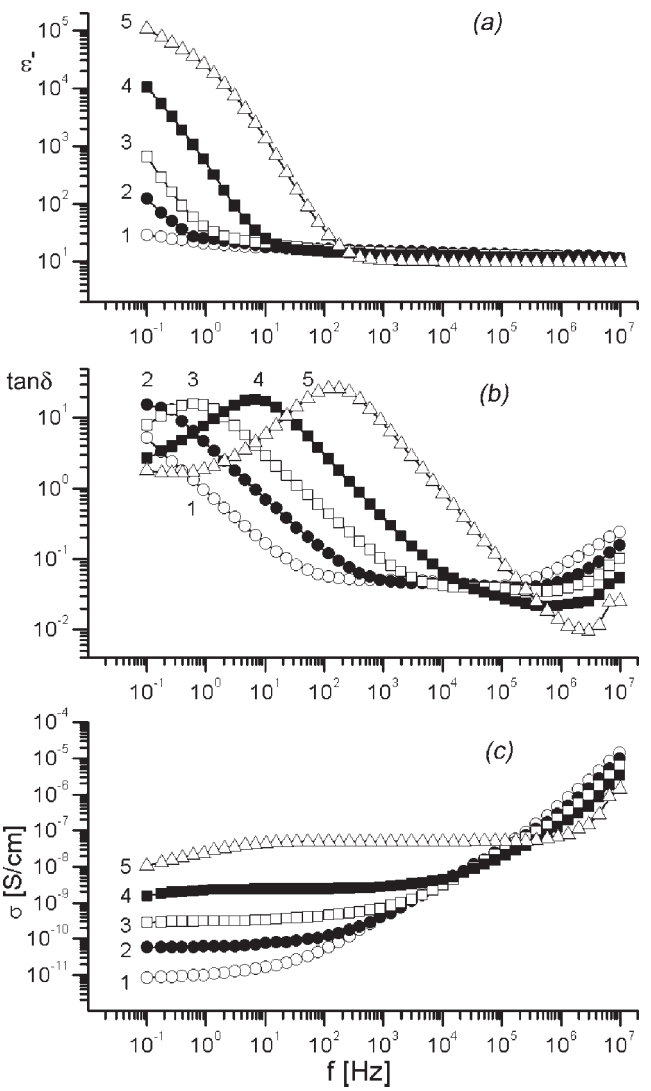

Figure 16 Frequency dependencies of the dielectric permittivity ε′ (a), tanδ (b), and conductivity σ (c) in the region of α-relaxation for VDF/HFP 93/7 copolymer at (1) 40°C, (2) 80°C, (3) 100°C, (4) 120°C, and (5) 150°C.

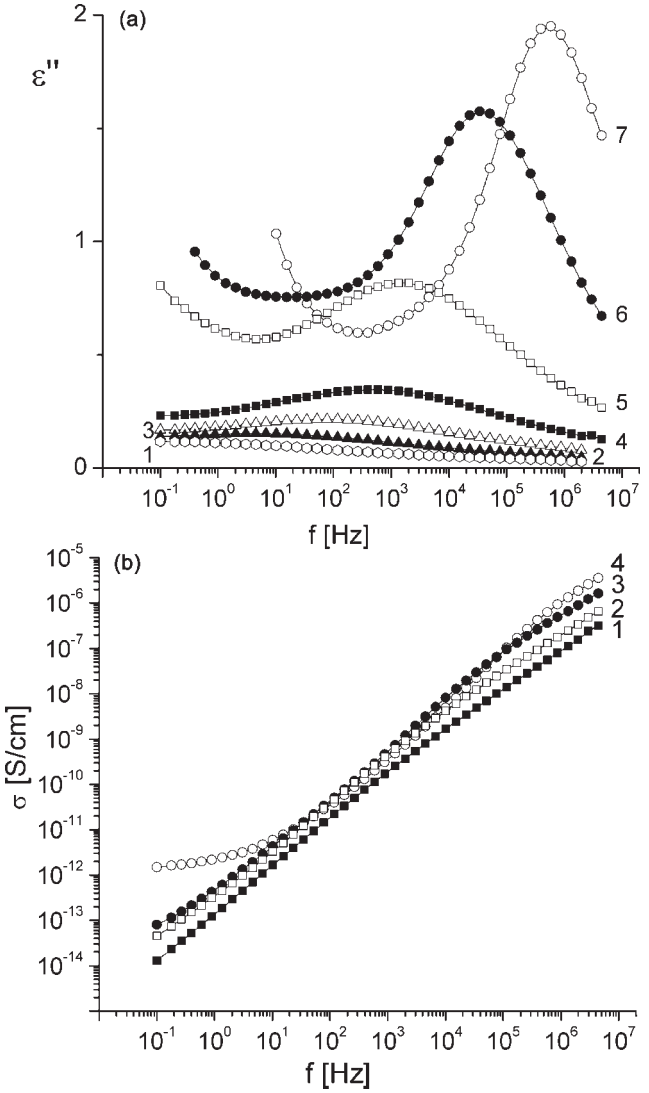

Figure 17 Frequency dependencies of the tanδ (a) and conductivity σ (b) in the region of α_a-relaxation for VDF/HFP 86/14 copolymer at (1) −40°C, (2) −20°C, (3) 0°C, and (4) 20°C.

microbrownian motion with high amplitudes of reorientation. It leads to the fact that crystals and amorphous phase will differ in dielectric permittivity and conductivity. Thus, in these crystalline polymers polarization of Maxwell–Wagner–Scillars type (MWS) can be observed.

This heterogeneity must be particularly expressed in considered copolymers. In fact, low glass transition temperature (see Table I) leads to small relaxation times $<10^{-6}$ s (Fig. 10) for mentioned segmental mobility at room temperatures. As movement of charges of ionogenic impurities is in the amorphous phase, the mobility of carriers is higher. This will cause a high difference in conductivity of considered phases. If α-process is related to the development of the space charge, the character of movement of free carriers appears to be sensitive to structural changes in the amorphous phase. From Figures 13 and 14 it follows that α-transition with relaxation times $\sim 10 \div 1$ s begins at temperatures of ferroelectric–paraelectric phase transition. It is known that the paraelectric phase is characterized by smaller density of chain package[2,4] and thus mobility of carriers will increase. From the same figures, it follows that melting leads to decrease in relaxation times of considered process. If it is connected with MWS relaxation, then there are peculiarities on frequency dependences of σ_{ac} that is demonstrated at Figures 15–18. In Figure 15 frequency behavior of σ in the region of α_c- and α_a-relaxations is shown for VDF/HFP copolymer with 7 mol % HFP. Conductivity increases with increase of frequency of electric field in all temperature range. The same behavior is observed for the copolymer with 14 mol % HFP (Fig. 17). From Figures 16 and 18 it fol-

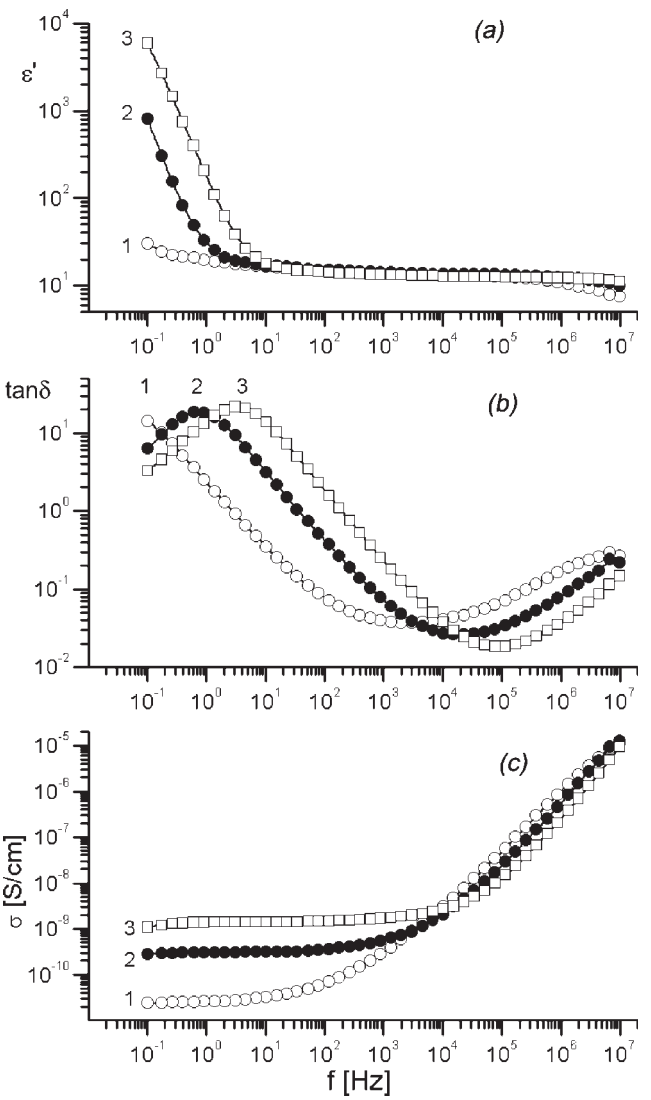

Figure 18 Frequency dependencies of the dielectric permittivity ε′(a), tanδ (b), and conductivity σ (c) in the region of α-relaxation for VDF/HFP 86/14 copolymer at (1) 40°C, (2) 60°C, and (3) 80°C.

lows that in temperature region of α-relaxation, however, there is a frequency range where conductivity is constant for both copolymers. Such behavior is typical for heterogeneous systems where components strongly differ on electric parameters.[79–83]

For discussion of data in considered systems[80–82,84–87] complex electric modulus $M^*(\omega)$ offered by authors of Refs. 88 and 89 is often used

$$M^*(\omega) = \frac{1}{\varepsilon^*(\omega)} = M' + iM'' = \frac{\varepsilon'}{\varepsilon'^2 + \varepsilon''^2} + i\frac{\varepsilon''}{\varepsilon'^2 + \varepsilon''^2} \tag{10}$$

In Figure 19 isothermal frequency dependencies of imaginary part of complex electric modulus, M'', in the region of α-relaxation, are shown for considered copolymers. The curves exhibit relaxation behavior.

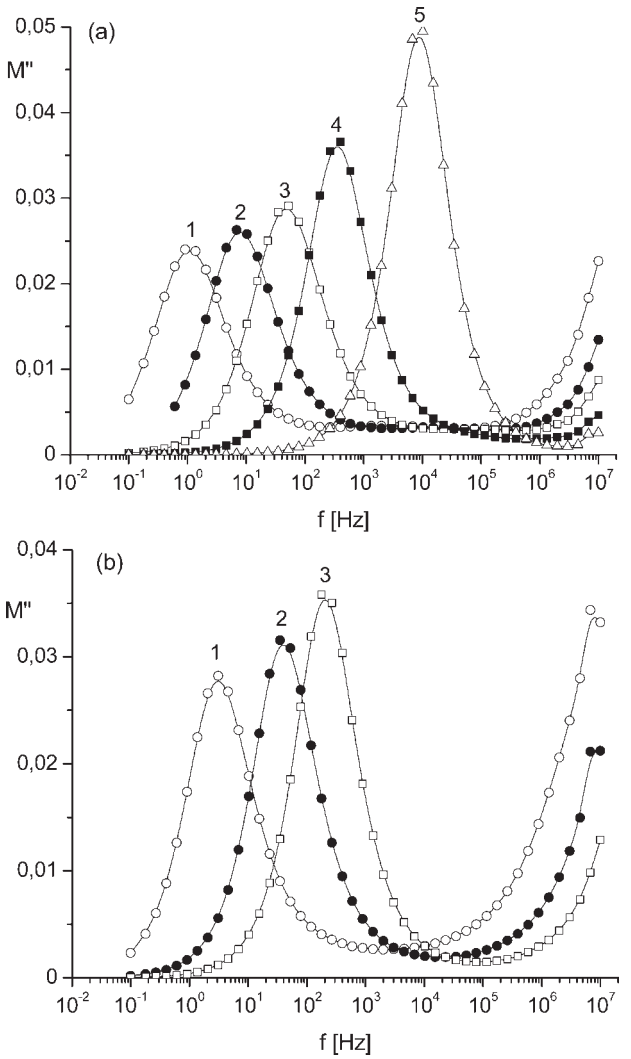

Figure 19 Frequency dependencies of the imaginary part of electric modulus M'' in the region of α-relaxation in 93/7 (a) and 86/14 (b) copolymers at (a): 60°C (1), 80°C (2), 100°C (3), and 140°C (4); (b): 40°C (1), 60°C (2), and 80°C (3).

Thus, formally, our experimental data are qualitatively predicted by MWS theory. The relaxation strength Δε and relaxation time τ of α-process can be written as

$$\Delta\varepsilon = (v/A)\varepsilon_a \tag{11}$$

$$\tau = \frac{\varepsilon_a \varepsilon_0}{A\sigma} \tag{12}$$

Here ε_0 is the electric constant, and ε_a is the dielectric permittivity of the matrix containing a volume fraction v of inclusions with conductivity σ and form-factor A. The melting of crystals can increase the heterogeneity in the system because trapped charges will be released. We assume that traps localized on crystals' surface predominantly immobilize ionogenic impurities. According to eq. (11), Δε is proportional to the volume fraction v of considered inclusions. From Figure 19 it follows that Δε increases with temperature, according to the prediction of MWS theory [eq. (11)]. Let us calculate the relaxation time according to eq. (12) at assumption of spherical particles ($A = 1/3$) with high conductivity σ (Figs. 16 and 18), imbedded in a matrix with $\varepsilon_a = 20$. Calculation shows that experimental values of τ, obtained from frequency dependences of tanδ, are by 1–2 orders higher than predicted by the eq. (11). From the other hand, if τ is calculated from $M''(\omega)$ dependences, there is a correspondence with accuracy of 30–40%.

Finally, let us stop on possibility of the third mechanism for explanation of α-relaxation. In Figures 16 and 18 dispersion curves of a real part of dielectric permittivity for considered transition in studied copolymers are shown. As seen, at low frequencies ε' reach high values that are not typical for relaxation processes considered earlier. Authors[16,19,23,90,91] have suggested that, with reference to PVDF, considered α-process should be connected with manifestation of electrode polarization. According to these papers, complex dielectric permittivity have polymer (p) and ionic (i) components:[92]

$$\varepsilon' = \varepsilon'_i + \varepsilon'_p \tag{13}$$

$$\varepsilon'' = \varepsilon''_i + \varepsilon''_p \tag{14}$$

Ionic components for real and imaginary parts are[92]

$$\varepsilon'_i = \frac{2v_0q^2}{dkT\pi^{0,5}}\left(\frac{D_0}{f}\right)^{3/2} \exp\left[-\left(\frac{3E_d}{2} + \frac{W}{2\varepsilon_0}\right)/kT\right] \tag{15}$$

$$\varepsilon''_i = \frac{2v_0q^2}{kT}\left(\frac{D_0}{f}\right) \exp\left[-\left(E_d + \frac{W}{2\varepsilon_0}\right)/kT\right], \tag{16}$$

where v_0 is the concentration of mobile ions with charge q_0, d is the thickness of the sample, D_0 is the

diffusion coefficient, f is the frequency of electric field, E_d is the activation energy of ionic diffusion, W is the dissociation energy of impurity molecules. Relations 15 and 16 predict occurrence of a high low-frequency dielectric dispersion.[90] According to the eq. (15) ε' value is inversely proportional to the sample thickness. Our preliminary data have qualitative agreement with such prediction. In this connection, there are reasons to connect discussed α-transition (Figs. 16 and 18) with electrode polarization process. It is known that it can be suppressed by blocking of electrodes.[93] It was made for PVDF, for example, by positioning PTFE film between the film and the electrode.[90] In our case, at temperatures below melting point part of crystals of α-phase, located on the interface with evaporated metal of an electrode, can be such blocking layer. At melting, the number of such crystals reduces, that is equivalent to decrease in degree of an electrode blocking. It is accompanied by increase of measured dielectric permittivity.[90] In our experiment (Figs. 16 and 18) we see the same. Process of melting in the investigated copolymers takes place in wide enough temperature interval (Figs. 13 and 14), and therefore the degree of electrode blocking will smoothly vary. In process of crystals' melting, double electric layer will develop on metal–polymer interface due to the ions present in the melt. It can lead to the sharp increase in dielectric permittivity (Figs. 13 and 14) that, in its turn, will lead to decrease in dissociation energy W of impurities in relations (15) and (16). Thus, one should expect additional increase in number of mobile carriers ν_0 in the system. It means that development of electrode polarization will have autocatalytic nature.

In this problem it is important to find out the nature of carriers forming space charge. According to authors of Ref. 94 there should be Na, Ca, Al, S, and Cl ions in PVDF. Their partial neutralization on electrodes, at authors' opinion, also leads to decrease of high-temperature dielectric characteristics of PVDF after its exposure in a static electric field.[22,94] From the other hand, H^+ and F^- ions, which appear from dissociation of HF molecules, should be carriers in considered polymers.[95] It is supposed that HF molecules are generated at high temperatures by the dehydrofluorination reactions

$$(\text{—}CH_2\text{—}CF_2\text{—}) \rightarrow HF + (\text{—}CH{=}CF\text{—}) \qquad (17)$$

Our data also point out indirectly the important role of H^+ and F^- carriers in considered α-relaxation process. Indeed, preliminary data show that change in metal of an electrode affects low-frequency dielectric permittivity values. It is possible to explain only by the supposition that namely fluorine ions can perform active interaction with Al.[95,96]

Correlation diagrams for α-transition are shown in Figure 10. The dependences obtained from temperature changes of σ_{dc}, $\tan\delta_m$, and M''_m are shown separately on an insert. One can see that relaxation times of given process can be approximated by Arrhenius equation to a first approach. It has allowed to calculate activation parameters for given process. They have been received from temperature–frequency dependences of $\tan\delta_m$ and listed in Table I. It is seen that conventional temperature of defreezing of α-transition (T') in VDF/HFP 93/7 copolymer is almost 40° higher than in a copolymer with 14 mol % HFP. It confirms once again that α-process is initiated by melting of crystals, since melting temperatures in both copolymers, according to Figure 2, differ approximately on as much. From the other hand, activation parameters of the given process differ essentially in considered copolymers. In Table I they are calculated from temperature–frequency dependences of $\tan\delta_m$. It is seen that increase of HFP content leads to decrease of activation enthalpy almost in 2 times. Activation entropy falls essentially more (more than by one order). According to relations 15 and 16, activation parameters of α-transition are controlled both by dissociation energy (W) of ionogenic impurities and by activation energy of diffusion (D_0) of appearing charges. If carriers move in amorphous phase, D_0 will be determined by parameters of microbrownian motion in it (α_a-process). From comparison of curves 2 and 2′ (Fig. 10) it is seen that above the room temperature (α-relaxation region) average frequencies of reorientation of segments and their activation energies are similar for both copolymers. Therefore, the parameters of diffusive transport are the same. On the other hand, higher fraction of CF_3 groups in

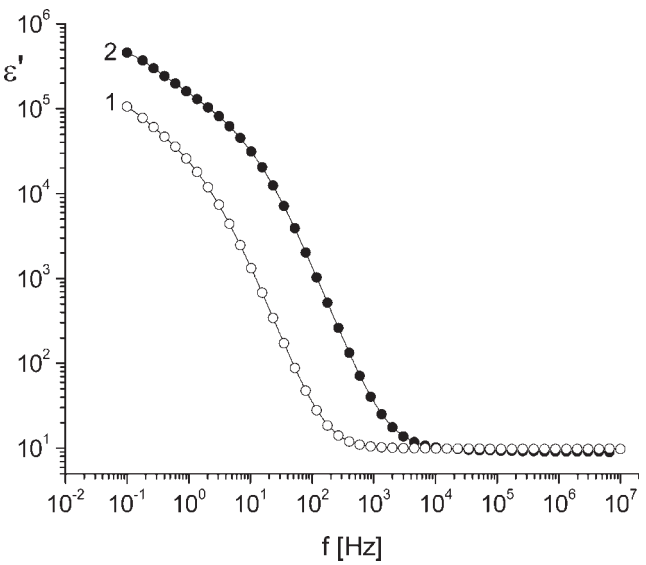

Figure 20 Frequency dependencies of the dielectric permittivity ε' in the region of α-relaxation (at 140°C) in 93/7 (1) and 86/14 (2) copolymers.

VDF/HFP copolymer of 86/14 content leads to increase of low-frequency dielectric permittivity (Fig. 20). This should manifest itself in decrease of dissociation energies W of ionogenic impurities. As a consequence, there is experimentally observable decrease of activation parameters of α-transition in this copolymer.

CONCLUSIONS

A number of transitions have been observed by dielectric method in copolymers of vinylidene fluoride with hexafluoropropylene. Local mobility below a glass transition point is not sensitive to the chemical composition of polymers. Characteristics of cooperative motion process at glass transition noticeably differ in copolymers with different HFP content. The qualitative explanation is given from the positions of modified Fox's equation, but the change of crystallinity must be considered. It has been found that increase of HFP content from 7 up to 14 mol % results in disappearance of α_c-relaxation. This is connected with decrease of volume fraction of crystals which size essentially decreases. Dielectric and thermal anomalies typical for ferroelectric phase transitions have been detected at 50–70°C. It is suggested that spontaneous polarization regions of nanometer size are localized in amorphous phase. It has been shown that the Curie temperature correlates with average density of chain packing in domains of amorphous phase. An intensive relaxation process connected with manifestation of space charge is observed in temperature region where DSC method detects melting of crystals. High dielectric permittivity values are connected with formation of a double electric layer on interface metal–polymer. The capacity of such layer is extensively controlled by formation of specific interactions between electrode metal (Al) and fluorine ions.

References

1. Wang, T. T.; Herbert, J. M.; Glass, A. M., Eds. The Application of Ferroelectric Polymers; Blackie: Glasgow, 1988.
2. Kochervinskii, V. V. Russ Chem Rev 1999, 68, 821.
3. Kochervinskii, V. V. Russ Chem Rev 1994, 63, 367.
4. Nalva, H. S., Ed. Ferroelectric Polymers—Chemistry, Physics and Applications; Marcel Dekker: New York, 1995.
5. Kochervinskii, V. V. Crystallogr Rep (Russia) 2003, 48, 649.
6. Kochervinskii, V. V. Polym Sci (Russia) 2003, 45, 1922.
7. Xiao, Q.; Zhou, X. Acta Polym Sinica 2003, 2, 139.
8. Kochervinskii, V. V. Russ Chem Rev 1996, 65, 865.
9. Kakutani, H. J Polym Sci Part A-2: Polym Phys 1970, 8, 1177.
10. Baird, M. E.; Blackburn, P.; Delf, B. W. J Mater Sci 1975, 10, 1248.
11. Startzev, O. V.; Perepechko, I. I.; Maliysheva, T. P. Vyisokomol Soed B (Russia) 1976, 18, 381.
12. Enns, J. B.; Simha, R. J Macromol Sci Phys 1977, 13, 11.
13. Osaki, S.; Kotaka, T. Rep Progr Polym Phys Jpn 1980, 23, 473.
14. Miyamoto, Y.; Miyaji, H.; Asai, K. J Polym Sci Polym Phys Ed 1980, 18, 597.
15. Sakamoto, R.; Abe, Y.; Yano, S. Rep Progr Polym Phys Jpn 1980, 23, 359.
16. Osaki, S.; Ishida, Y.; Yamafuji, K. Polym J 1980, 12, 171.
17. Das-Gupta, D. K.; Doughty, K. Ferroelectrics 1980, 28, 307.
18. Das-Gupta, D. K.; Doughty, K. Ferroelectrics 1981, 32, 69.
19. Osaki, S.; Kotaka, T. Ferroelectrics 1981, 32, 1.
20. Arisawa, H.; Yano, O.; Wada, Y. Ferroelectrics 1981, 32, 39.
21. Koizumi, N.; Hagino, J.; Murata, Y. Ferroelectrics 1981, 32, 141.
22. Oka, Y.; Koizumi, N. Polym J 1982, 14, 869.
23. Cebe, P.; Grubb, D. T. Macromolecules 1984, 17, 1374.
24. Koizumi, N.; Haikawa, N.; Habuka, H. Ferroelectrics 1984, 57, 99.
25. Abe, Y.; Kakizaki, M.; Hideshima, T. Ferroelectrics 1984, 57, 9.
26. Furukawa, T.; Ohuchi, M.; Chiba, A.; Date, M. Macromolecules 1984, 17, 1384.
27. Abe, Y.; Kakizaki, M.; Hideshima, T. Jpn J Appl Phys 1985, 24, 208.
28. Hahn, B.; Wendorff, J. H.; Yoon, D. Y. Macromolecules 1985, 18, 718.
29. Hahn, B.; Herrmann-Schonher, O.; Wendorff, J. H. Polymer 1987, 28, 201.
30. Kuleshov, I. V.; Bartenev, G. M. Acta Polym 1988, 39, 288.
31. Furukawa, T.; Tajitsu, Y.; Zhang, X.; Johnson, G. E. Ferroelectrics 1992, 135, 401.
32. Teyssedre, G.; Grimau, M.; Bernes, A.; Martinez, J. J.; Lacabanne, C. Polymer 1994, 35, 4397.
33. Kochervinskii, V. V.; Baranov, A. I. Izvestiya RAN Phys (Russia) 1997, 61, 283.
34. Kochervinskii, V. V. Polym Sci A (Russia) 2000, 42, 1077.
35. Kochervinskii, V. V. Polym Sci A (Russia) 2002, 44, 20.
36. Kochervinskii, V. V. Polym Sci A (Russia) 2002, 44, 695.
37. Kochervinskii, V. V. Polym Sci A (Russia) 2002, 44, 1137.
38. Takahashi, Y.; Miyaji, K. Macromolecules 1983, 16, 1789.
39. Carbeck, J. D.; Rutledge, G. C. Macromolecules 1996, 29, 5190.
40. Danch, A.; Osoba, W. J Therm Anal Cal 2003, 72, 641.
41. Pak, J.; Pyda, M.; Wunderlich, B. Macromolecules 2003, 36, 495.
42. Xu, H.; Cebe, P. Macromolecules 2004, 37, 2797.
43. Huo, P.; Cebe, P. Macromolecules 1992, 25, 902.
44. Huo, P.; Cebe, P. J Polym Sci Part B: Polym Phys 1992, 30, 239.
45. Natesan, B.; Xu, H.; Ince, B. S.; Cebe P. J Polym Sci Part B: Polym Phys 2004, 42, 777.
46. Kochervinskii, V. V. Polym Sci (Russia) 1998, 40, 1020.
47. Kochervinskii, V. V.; Sul'yanov, S. N. Fiz Tv Tela (Russia) 2006, 48, 1016.
48. Latour, M.; Anis, K. IEEE Trans Elect Insul 1993, 28, 111.
49. Kim, K. M.; Park, N.-G.; Ryu, K. S.; Chang, S. H. Polymer 2002, 43, 3951.
50. Moggi, G.; Bonardelli, P.; Bart, J. C. J Polym Bull 1982, 7, 115.
51. Moggi, G.; Bonardelli, P.; Monti, C.; Bart, J. C. J Polym Bull 1984, 11, 35.
52. Schoenhals, A.; Kremer, F.; Schlosser, E. Phys Rev Lett 1991, 67, 999.
53. Hofmann, A.; Kremer, F.; Schoenhals, A.; Fischer, E. W. In Disorder Effects on Relaxational Processes; Richert, R.; Blumen, A., Eds.; Springer: Berlin, 1994; pp 309–331.
54. Skinner, J. L.; Park, Y. H. Macromolecules 1984, 17, 1735.
55. Sy, J.-L.; Mansfeld, M. L. Polymer 1988, 29, 987.
56. Leonard, C.; Monnerie, H. L.; Micheron, F. Polym Bull 1984, 11, 195.
57. Loufakis, K.; Wunderlich, B. Macromolecules 1987, 20, 2474.
58. El Mohajir, B.-E.; Heymans, N. Polymer 2001, 42, 5661.
59. Ajroldi, G.; Pianca, M.; Fumagalli, M.; Moggi, G. Polymer 1989, 30, 2181.
60. Mekhilef, N. J Appl Polym Sci 2001, 80, 230.
61. Bonardelli, P.; Moggi, G.; Turturro, A. Polymer 1986, 27, 905.

62. Kalika, D. S.; Krishnaswamy, R. K. Macromolecules 1993, 26, 4252.
63. Fukao, K.; Miyamoto, Y. J. Non-crystal Solids 1994, 172–174, 365.
64. Ezquerra, T. A.; Liu, F.; Boyd, R. H.; Hsiao, B. S. Polymer 1997, 38, 5793.
65. Fukao, K.; Miyamoto, Y. Polymer 1993, 34, 238.
66. Wunderlich, B.; Czornyi, G. Macromolecules 1977, 10, 906.
67. Lau, S.-F.; Wunderlich, B. J. Polym Sci Part B: Polym Phys 1984, 22, 379.
68. Cross, L. E. Ferroelectrics 1994, 151, 305.
69. Maeda, K.; Tasaka, S.; Inagaki, N. Jpn J Appl Phys 1991, 30, 716.
70. Koizumi, N.; Murata, Y.; Tsunashima, H. IEEE Trans Elec Insul 1986, 21, 543.
71. Tashiro, K.; Takano, K.; Kobayashi, M.; Chatani, Y.; Tadokoro, H. Ferroelectrics 1984, 57, 297.
72. Kochervinskii, V. V.; Sul'yanov, S. N.; Dembo, K. A. Polymer 2007, 48, to appear.
73. Budhane, S. P.; Shirodkar, V. S. J Appl Polym Sci 1997, 64, 225.
74. Wang, T. T.; Takase, Y. J Appl Phys 1987, 62, 3466.
75. Nakamura, T.; Takashiga, M.; Terauchi, H.; Miura, Y.-I.; Lawless, W. N. Jpn J Appl Phys 1984, 23, 1265.
76. Kotaka, T. K.; Adachi, K. Macromol Symp 1997, 124, 3.
77. Kyritsis, A.; Pissis, P.; Mai, S.-M.; Booth, C. Macromolecules 2000, 33, 4581.
78. Hayakawa, T.; Adachi, K. Polymer 2001, 42, 1725.
79. Hayard, D.; Pethrick, R. A.; Siriwittayakorn, T. Macromolecules 1992, 25, 1480.
80. Pissis, P.; Kyritsis, A. Solid State Ionics 1997, 97, 105.
81. Kanapitsas, A.; Pissis, P.; Estrella, A. G. Eur Polym J 1999, 35, 923.
82. Pissis, P.; Kyritsis, A.; Georgoussis, G.; Shilov, V. V.; Shevchenko, V. V. Solid State Ionics 2000, 136/137, 255.
83. Polizos, G.; Kyritsis, A.; Pissis, P.; Shilov, V. V.; Shevchenko, V. V.; Solid State Ionics 2000, 136/137, 1139.
84. Diaz Calleja, R. J Non Cryst Solids 1994, 172–174, 1413.
85. Wagner, H.; Richert, R. Polymer 1997, 38, 5801.
86. Leon, C.; Lucia, M. L.; Santamaria, J. Phil Mag B 1997, 75, 629.
87. Mudarra, M.; Diaz Calleja, R.; Belana, J.; Canadas, J. C.; Diego, J. A.; Sellares, J.; Sanchis, M. J. Polymer 2001, 42, 1647.
88. Macedo, P. B.; Moynihan, C. T.; Bose, R. Phys Chem Glass 1972, 13, 171.
89. Yamamoto, K.; Namikawa, H. Jpn J Appl Phys 1988, 27, 1845.
90. Osaki, S.; Uemura, S.; Kotaka, T.; Report Progr Polym Phys Jpn 1980, 23, 469.
91. Uemura, S. J Polym Sci Polym Phys Ed 1972, 10, 2155.
92. Uemura, S. J Polym Sci Polym Phys Ed 1974, 12, 1177.
93. Coelho, R. Revue Phys Appl 1983, 18, 137.
94. Osaki, S.; Uemura, S.; Ishida Y. J Polym Sci Polym Phys Ed 1971, 9, 585.
95. Felix-Vandorpe, M.-C.; Maitrot, M.; Ongaro, R. J Phys D: Appl Phys 1985, 18, 1385.
96. Wu, P. K.; Yang, G.-R.; Ma, X. F.; Lu, T.-M. Appl Phys Lett 1994, 65, 508.
97. Ogura, H.; Tohriyama, S.; Hanaki, A.; Sasaki, S.; Kase, K.; Chiba, A. Jpn J Appl Phys 1991, 30, 2819.